The Journal of Experimental Biology 215, 1151-1161

doi:10.1242/jeb.068080

RESEARCH ARTICLE

A buckling region in locust hindlegs contains resilin and absorbs energy when jumping or kicking goes wrong

T. G. Bayley, G. P. Sutton and M. Burrows*

Department of Zoology, University of Cambridge, Cambridge CB2 3EJ, UK

*Author for correspondence (mb135@hermes.cam.ac.uk)

Accepted 6 December 2011

SUMMARY

If a hindleg of a locust slips during jumping, or misses its target during kicking, energy generated by the two extensor tibiae muscles is no longer expended in raising the body or striking a target. How, then, is the energy in a jump (4100–4800 μJ) or kick (1700 μJ) dissipated? A specialised buckling region found in the proximal hind-tibia where the bending moment is high, but not present in the other legs, buckled and allowed the distal part of the tibia to extend. In jumps when a hindleg slipped, it bent by a mean of 23±14 deg at a velocity of 13.4±9.5 deg ms^{-1}; in kicks that failed to contact a target it bent by 32±16 deg at a velocity of 32.9±9.5 deg ms^{-1}. It also buckled 8.5±4.0 deg at a rate of 0.063±0.005 deg ms^{-1} when the tibia was prevented from flexing fully about the femur in preparation for both these movements. By experimentally buckling this region through 40 deg at velocities of 0.001–0.65 deg ms^{-1}, we showed that one hindleg could store about 870 μJ on bending, of which 210 μJ was dissipated back to the leg on release. A band of blue fluorescence was revealed at the buckling region under UV illumination that had the two key signatures of the elastic protein resilin. A group of campaniform sensilla 300 μm proximal to the buckling region responded to imposed buckling movements. The features of the buckling region show that it can act as a shock absorber as proposed previously when jumping and kicking movements go wrong.

Supplementary material available online at http://jeb.biologists.org/cgi/content/full/215/7/1151/DC1

Key words: energy storage, fluorescent proteins, campaniform sensilla.

INTRODUCTION

Animals that produce fast and powerful movements are liable to cause damage to their bodies if an unpredictable event occurs, especially if underlying muscular and skeletal material has a low safety factor (the ratio between the standard operating forces of the system and the forces that would cause its parts to break). During running, rowing, baseball, cricket and ballet dancing, humans generate high forces that can fracture arm, leg or rib bones (Bennell and Brukner, 2005; Bennell and Brukner, 1997; Jones, 2006; Pohl et al., 2008). Baseball pitchers occasionally fracture their humerus during a pitch (Branch et al., 1991; Polu et al., 1999), despite the peak torque involved being about half the theoretical torsional strength of the humerus; the safety factor is 2 (Sabick et al., 2004). But fatigue in the bones and muscles both increases stresses on the bones and reduces their ability to resist them (Jones, 2006).

Relative to body size, some of the fastest and most powerful movements are those of the legs of jumping insects. For example, froghoppers and planthoppers (both Hemiptera) accelerate in less than 1 ms to take-off velocities of around 5 m s^{-1} (Burrows, 2003; Burrows, 2006; Burrows, 2009). The much heavier locusts (Orthoptera) achieve take-off velocities of 3 m s^{-1} (Bennet-Clark, 1975; Brown, 1967) and the safety factor of their hindlegs is estimated to be no more than 1.2 (Bennet-Clark, 1975). This means that even under optimal conditions, the forces required for jumping or kicking come within 20% of damaging the hindlegs. This brings locusts closer to breaking their legs during a jump than baseball pitchers come to breaking their arms during a pitch. Indeed, the tendon of the main muscle that extends their hindlegs can snap under experimentally imposed loads similar to those that occur during natural jumping (Bennet-Clark, 1975).

How do insects operating near their structural limits avoid damage to their jumping machinery? In locusts, a specialised region of the proximal hind-tibia (the plane of weakness, now renamed by us as the buckling region), not found on the other legs, has been suggested to absorb excess kinetic energy when it bends (Heitler, 1977). Bending has so far only been demonstrated during kicks that fail to contact an intended target (Burrows and Morris, 2001). Heitler showed that along this plane of weakness, the ventral cuticle has no lamellations or growth layers visible under a scanning electron microscope, and the exocuticle and endocuticle are heavily sclerotised (Heitler, 1977). By contrast, its dorsal surface possesses thick and separate striations, suggesting a difference in shear strength between the lamellae. Heitler suggested that buckling at this region could be caused by these laminae sliding past each other, a process facilitated by a reduction in the cross-linkage between inter-laminar proteins and chitin microfibrils (Heitler, 1977). He searched for, but did not find, the elastic protein resilin here. Heitler (Heitler, 1977) proposed three functions for this region: first, to reduce the inertial shock to the femur when the tibia reaches full extension in a kick; second, to allow the tibia to flex fully about the femur in preparation for a kick; and third, to focus cuticular strain onto a nearby group of campaniform sensilla and the subgenual organ, as has also been proposed for a similar arrangement in the tibia of a termite (Howse, 1965).

To test the proposals of Heitler about the function of the plane of weakness (Heitler, 1977), we used a combination of high speed

imaging, mechanics and neurophysiology. We analysed natural jumping when a hindleg slips, and kicking when a target is missed, and show that buckling can occur during both movements. Buckling did not occur when the tibia was flexed in preparation for a jump, unless flexion was impeded. We show that buckling is capable of dissipating energy, and thereby reduces the energy that would have to be absorbed by structures such as the joints. We also show that this buckling region contains a band of resilin that may help in energy storage and enable the original shape of the tibia to be restored after buckling. Finally, of the sense organs close to this region, we show that a group of campaniform sensilla responds to buckling movements.

MATERIALS AND METHODS

Adult male and female, gregarious-phase locusts (*Schistocerca gregaria* Forskål) were analysed from our culture in Cambridge. All measurements were made on adults 10–17 days post-final moult; the cuticle of the proximal metathoracic tibia reaches its final hardness 3 days post-moult (Hillerton et al., 1982). Lengths of the hind-tibiae of fixed specimens were measured against a ruler to an accuracy of 0.1 mm on images captured with a digital camera attached to a Leica MZ16 microscope (Wetzlar, Germany). Body mass was determined to an accuracy of 0.1 mg with a Mettler Toledo AB104 balance (Beaumont Leys, Leicester, UK).

Locusts jumped naturally from a wooden platform either spontaneously or when the abdomen was tickled with a fine paintbrush. Images of these jumps were captured at rates of 1000 s^{-1} with an exposure time of 0.066 ms (supplementary material Movie 1) using a Photron Fastcam 1024 PCI camera (Photron Europe Ltd, High Wycombe, Bucks, UK). Kicking movements were elicited from locusts restrained ventral surface uppermost in Plasticene® with the tibia and tarsus of the right hindleg able to move freely. Images were captured at rates of 5000 s^{-1} with exposure times of 0.1 or 0.2 ms (supplementary material Movie 2). All images were recorded directly to a computer. The fastest kick by each locust was measured frame by frame from when the tibia started to extend until it was stationary. The velocity of the kicks was quantified from polynomials fitted to the data in Mathematica 5.0 (Wolfram Research Inc., Champaign, IL, USA). In a further set of 5 locusts, with 5 kicks from each analysed, the buckling region was painted with hard nail polish to prevent it from bending (supplementary material Movie 3). The kinematics of kicks were compared between locusts with and without nail polish present.

The forces needed to buckle the region, and hence the energy that could be absorbed by it, were measured in isolated hindlegs bent with a servo-motor (Aurora Scientific, 305B-LR, Aurora, ON, Canada). The motor was positioned 12 mm distal to the buckling region and calibrated to induce 40 deg bending of this region. Velocities were presented at 0.001 to 0.65 deg ms^{-1} in six steps using custom-written scripts in Spike2 (version 7) and a CED 1401 A/D converter (Cambridge Electronic Design, Cambridge, UK). Measurements of force were unreliable at higher velocities. Changes in velocity were applied in a random sequence for each locust at 5 s intervals to control for possible changes in material properties of the tibia over the course of the experiment. Comparisons were also made between a 0.001 deg ms^{-1} bend given at the beginning and end of each set of trials. The forces exerted back onto the servo-motor were recorded simultaneously in Spike2 at a sampling rate of 300 Hz. This force was then converted to a torque and work was derived as torque multiplied by the change in angle. Measurements of the torque required to bend the tibia, and that exerted back onto the servo-motor on release, were fitted to polynomial distributions in Mathematica 5.0. Integrating these distributions gave the energy absorbed and dissipated by the buckling region at the range of velocities tested. To assess whether permanent structural changes occurred during buckling, the energy absorption properties were tested over a 24 h period.

To analyse the anatomy of the proximal part of the hind-tibia, images of intact legs of live locusts were taken in air with a Nikon DXM 1200 digital camera mounted on a Leica MZ16 stereo microscope. Dried specimens cleaned with ethanol or acetone were sputter-coated with gold and examined in an XL-30 FEG scanning electron microscope (Philips, Eindhoven, The Netherlands). To test for the presence of the elastic protein resilin, the proximal tibia and femoro-tibial (FT) joint were viewed in locust saline (Usherwood and Grundfest, 1965) with an Olympus BX51WI compound microscope through Olympus MPlan 5×/0.1 NA and MPlan10×/0.25 NA objectives under ultraviolet (UV) or white epi-illumination. Longitudinal sections cut along the dorsal and lateral midlines were also analysed. UV light was provided from an X-cite series 120 metal halide light source with 350–407 nm incident light isolated with a DAPI-5060B Brightline filter (Semrock, Rochester, NY, USA) with sharp-edged (1%) transmission bands. Transmitted light was filtered from 413 to 483 nm with a dichroic beam splitter with a similarly sharp-edged cut-off. These wavelength bands correspond to the absorbance and emission peaks of resilin (Andersen and Weis-Fogh, 1964). An identifiable feature of the fluorescence of resilin is its sensitivity to pH (Andersen, 1963; Neff et al., 2001). Accordingly, the bathing saline was altered to pH 2 with 2 mol l^{-1} hydrochloric acid, and pH 12 with 2 mol l^{-1} sodium hydroxide. Camera gain and exposure time were held constant. Images were captured under transmitted and UV light with a MicroPublisher 5.0 digital camera (QImaging, Marlow, Bucks, UK) and superimposed in Canvas 11 (ACD Systems of America, Miami, FL, USA).

To test directly the proposal by Heitler that a group of campaniform sensilla on the proximal tibia could monitor buckling of this region (Heitler, 1977), the responses of their sensory neurons were recorded extracellularly from leg nerve N5B2 to which they project (Burrows and Pflüger, 1988). An isolated hindleg was used to avoid the signal being confounded by motor neurons. Nerves and sensory neurons distal to the buckling region were destroyed by removing the distal-most tip of the tibia and reaming the remaining interior surface with an insect pin as far proximal as the buckling region. After this procedure, mechanical stimulation of receptors distal to the buckling region failed to evoke spikes in N5B2. Proximal to the buckling region, an individual campaniform sensillum, also with projections to N5B2 (Burrows and Pflüger, 1988), was destroyed with a pin. The response of the subgenual organ, mentioned by Heitler as possibly monitoring bending of the buckling region (Heitler, 1977), was not recorded as its axons run in a different leg nerve (N5B1). For recording, N5B2 was exposed between the extensor and flexor tibiae muscles in the distal femur and hooked onto a pair of 100 µm diameter silver wires, insulated but for their tips, which were then coated with a mixture of mineral oil and Vaseline®. Nerve recordings were digitised at sampling rates of 16 kHz using a CED 1401 A/D converter. To identify the spikes that were generated by the group of campaniform sensilla in these recordings, a probe was made from a fine insect pin similar in size to an individual sensillum. Probing on, or very close to, the sensilla elicited spikes of three different amplitudes that were large relative to background. Forces of 10–100 mN were used, which are similar to those used in assessing the responses of cockroach campaniform sensilla (Spinola and Chapman, 1975).

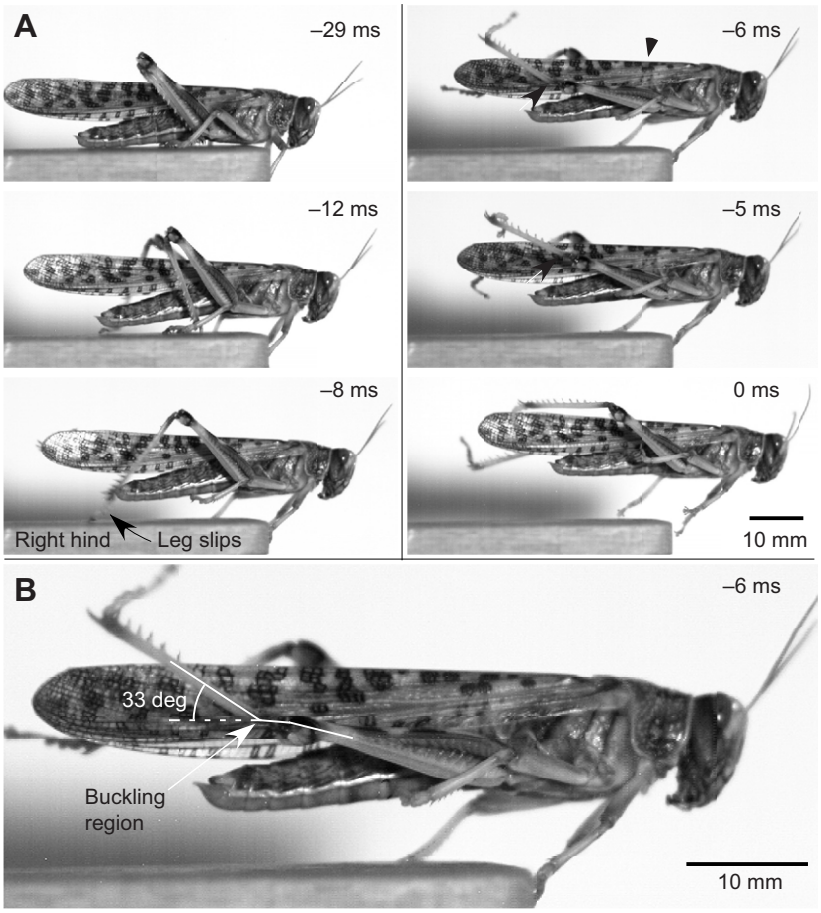

Fig. 1. Selected images of a jump by a male locust. (A) At the start of the jump, the tibiae of both hindlegs were fully flexed about the femora. Both tibiae then extended progressively, but before take-off, the right hindleg slipped (black arrow in frame –8 ms) and buckled (white arrows in frames –6 ms and –5 ms). Take-off occurred at time 0 ms. (B) An enlarged frame at –6 ms to show the right hind-tibia bent at the buckling region (white arrow) distal to the femoro-tibial (FT) joint. The angle of tibial bending is indicated. Images were captured at a rate of 1000 s^{-1} at the times indicated and are arranged in two columns.

The hind-tibia was bent using a McLennan servo-motor and gearbox (Radio Spares, Corby, Northants, UK) attached to an insect pin the same size as the internal diameter of the hollowed-out tibia into which it was inserted. To allow controlled buckling, and to ensure that the FT joint and femur remained stationary, the tibia was clamped between the FT joint and the group of sensilla. On clamping the tibia in this way, one sensillum produced tonic spikes that adapted to zero in around 30 s. To test the effect of the clamp on the responses of the group of sensilla, recordings were made before and after it was applied. No qualitative differences could be detected during imposed buckling but when the tibia was returned to its unbent position, the same sensillum produced tonic spikes that again adapted within 30 s. The servo-motor was driven by a custom-built function generator, or by a CED 1401 A/D converter using scripts written in Spike2. Stimuli were given in square, triangular or ramp-and-hold waveforms of controlled amplitude (2–16 deg) and velocity (0.002–0.3 deg ms^{-1}). The ramp-and-hold stimulus was separated into 5 sections for analysis: lead-in (1 s before stimulus onset), ramp, hold, release and lead-out (1 s after stimulus offset). The stimuli were repeated at 5 min intervals at which we recorded no differences in the sensory responses to buckling. The amplitudes of bending were similar to those that occur during natural kicking. The velocity of the movements was similar to that recorded during the co-contraction phase of kicking, when a stop was placed between the tibia and femur to prevent full flexion. The fastest velocity that could be achieved with step functions applied to this servo-motor was 0.3 deg ms^{-1}, meaning that the velocity reached at the end of a kick could not be simulated. Spikes were sorted by principal component analysis (using Spike2 WaveMark utility) and counted in 100 ms bins. The maximum spike rate varied between individual locusts, so that the value used was normalised to the maximum spike rate of all stimulus components.

To test for normality in all data, a Shapiro–Wilk test was used. Welch two-sample *t*-tests were used to determine significance if data were distributed normally and Mann–Whitney *U*-tests were used when they were not. For comparison between multiple groups, Kruskal–Wallis (K–W) tests were used. For regression analysis, ANOVA tests of the residuals were used. Significance was assigned with $P<0.05$, and adjusted with a Bonferroni–Dunn procedure to correct for multiple comparisons. Data are presented as means ± s.d. All experiments were carried out at a temperature of 22–24°C.

RESULTS

Natural jumping and kicking movements

When a locust jumped successfully, the rapid extension of the tibia about the femur was closely synchronised between the two hindlegs, and provided the energy for its propulsion from the platform. The movement was completed in 20–30 ms (24 locusts, 12 of each sex) and reached a maximum extension of 170–180 deg, achieved at the time of take-off. The hind-tibiae remained straight, despite their long length and narrow diameter, both during the preparatory co-contraction phase when the tibia was flexed about the femur, and during the subsequent rapid extension of the leg. Sometimes when jumping, the tarsus of a hindleg slipped and the tibia then bent at the buckling region (Fig. 1; see supplementary material Movie 1).

The motor pattern for kicking is very similar to that of jumping, also involving a preparatory co-contraction phase followed by a rapid extension of the hind-tibia (Burrows and Morris, 2001; Heitler and

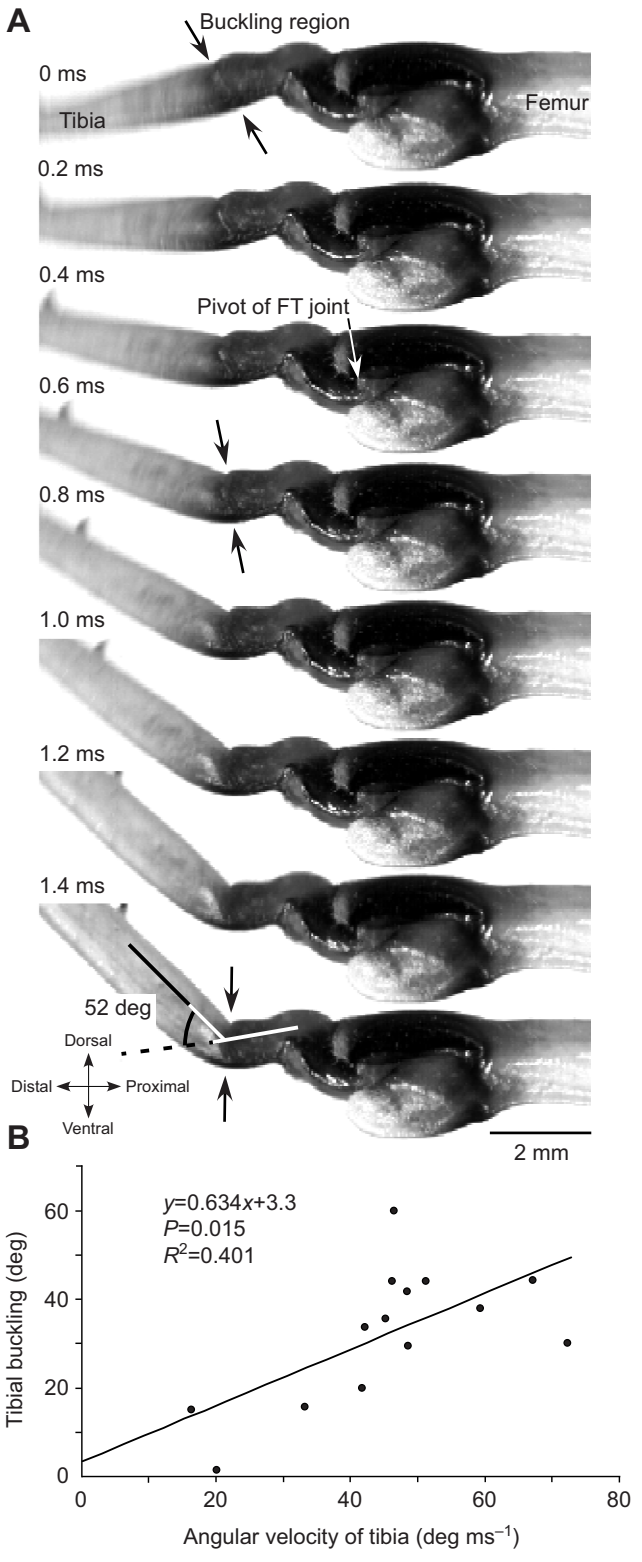

Fig. 2. Buckling of the right hind-tibia of a locust during a kick that missed its target. (A) Selected images of the kick at the times indicated. The image at the top represents the normal extent of tibial extension and is called time 0 ms. The tibia then began to bend at the buckling region (black arrows) distal to the pivot of the tibia with the femur (white arrow). Images were captured at a rate of 5000 s^{-1}. (B) Plot of the mean angular velocity of the tibia of 14 locusts during 68 kicks (1–8 kicks per locust), and the resulting buckling of the tibia.

Burrows, 1977a). Kicks recorded here most frequently involved the rapid movement of one hindleg, although co-ordinated kicks by both hindlegs were occasionally observed. As in jumping, the tibia remained straight during the preparatory co-contraction phase when the tibia was flexed about the femur. A kick was faster than a jump, with full extension achieved in 5 ms (Burrows and Morris, 2001). Sometimes a kick failed to meet a target and then the tibia bent at the buckling region when it reached full extension (Fig. 2A; see supplementary material Movie 2).

Jumping

To calculate the energy in a jump, the length and mass of the tibia were recorded. The mean length of an adult tibia was 20.9±0.5 mm in 12 females and 19.3±1.2 mm in 12 males. The diameter, which was similar along its entire length, was 0.96±0.21 mm in both sexes. In adult females the hind-tibia had a mass of 20±4.5 mg and the hind-tarsus 2.4±1.1 mg. In males the comparable masses were 16±1.8 mg and 2.1±0.5 mg. The mass of a female locust was 1.6±0.2 g and that of a male 1.1±0.1 g. During natural jumping, females achieved take-off velocities of 2.4±0.4 m s^{-1} and males 2.7±0.2 m s^{-1} (mean of means of 3 jumps by each locust). Accordingly, females expended 4800±2000 μJ of energy in a jump, whereas males expended 4100±900 μJ. The angular velocity of the tibia during a jump was 2.4±0.4 deg ms^{-1} (pooled data from 12 females and 12 males, 3 jumps each).

In jumps when a hindleg slipped, the force generated by that leg had only to accelerate the light weight of the tibia and tarsus, and not the weight of the whole body (Fig. 1A, Fig. 3A). As a consequence, the angular velocity of the tibia increased to 32.7±7.4 deg ms^{-1} (the fastest jump by each of 5 locusts) (Fig. 1A). The slippage reliably caused the tibia to buckle at the buckling region, about 3 mm distal to the FT joint (Fig. 1B). The angle of tibial buckling (Fig. 1B) ranged from 2 to 38 deg (mean 23±14 deg in single jumps by 8 locusts), extending at velocities of 13.4±9.5 deg ms^{-1} (5 locusts from the same set, 1 jump each). Once the tibia reached full extension, it showed a rebound flexion and a further smaller extension that was not accompanied by bending of the tibia at its buckling region (Fig. 3A). During the initial rapid extension of the tibia, the tarsus also levated fully about the tibia, and its segments curled (see Fig. 1A, –5 ms frame).

Kicking

As predicted by Heitler (Heitler, 1977), no buckling occurred when the tibia was flexed about the femur during the co-contraction preceding a kick (25 kicks in 11 locusts, 1–4 kicks each) unless a Plasticine® stop was placed between the tibia and femur to prevent full flexion. Then, the tibia buckled by 8.5±4.0 deg at an angular velocity of 0.063±0.005 deg ms^{-1} (13 kicks, 1–3 kicks by each of 5 locusts).

If a kick missed its target, the velocity of the tibia reached 46±15 deg ms^{-1} with a mean deformation at the buckling region of 32±16 deg (Fig. 2A, mean of means of 68 kicks by 14 locusts, 1–8 kicks for each locust). The angular velocity of buckling was 32.9±9.5 deg ms^{-1} on extension and 14.0±3.0 deg ms^{-1} on recoil (mean of means from 18 kicks in 11 locusts, 1–3 kicks by each locust), a difference that was significantly different ($P<0.0001$, $t=6.0$, t-test). The extent of buckling was dependent on the peak velocity of the tibia during kicking ($P=0.015$, $R^2=0.401$, ANOVA of residuals) (Fig. 2B). Tibial extension was completed in 5 ms and such was its velocity that when it rebounded from full extension it underwent a series of damped oscillations (Fig. 3B). There was insufficient time between these oscillations for them to be under

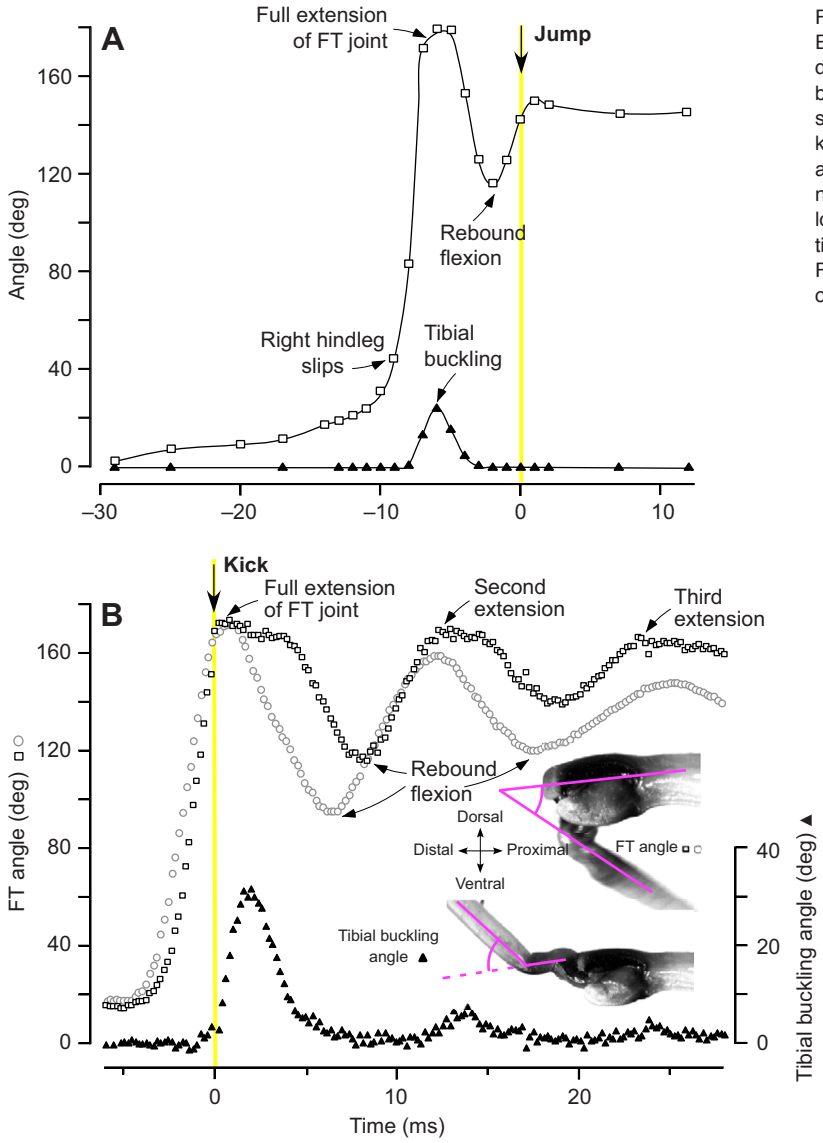

Fig. 3. Tibial buckling during natural behaviour. (A) Jumping. Example plot of the changes in the FT joint angle (open squares) during a jump powered by both hindlegs. The right hind-tibia buckled (angle of buckling plotted as filled triangles) after it slipped before take-off. (B) Kicking. A similar example plot for a kick by a right hindleg (FT joint angle, open squares) and the angle of buckling (filled triangles) of the proximal tibia during a natural kick. The grey circles show a second kick by a different locust in which buckling was prevented by painting the proximal tibia with nail varnish. The inset pictures show how the plotted FT joint angle and buckling angle of the proximal tibia were obtained.

neural control (see Discussion). To simulate striking a target, a stop was positioned in the path of the tibia to prevent it from extending beyond 90–140 deg. The hind-tibia then remained rigid, with the angle about the buckling region not significantly different from at rest (P=0.42, t=0.84, t-test, 13 kicks, 1–2 kicks by each of 10 locusts).

Applying a coat of nail varnish to the proximal tibia successfully prevented buckling from occurring in an experimental group of 5 locusts (4–5 kicks each; see supplementary material Movie 3). No difference was observed between the initial angular velocity of the tibia during kicks of the treated group (52.0±11.0 deg ms^{-1}) and those of an untreated control group (52.6±11.4 deg ms^{-1}, 12 locusts; P=0.32, t=1.02, t-test) (Fig. 3B). The first rebound flexion of the tibia, however, occurred at a significantly higher angular velocity in treated locusts; 25±8 deg ms^{-1} (4–5 kicks by each of 5 locusts) compared with 16±5 deg ms^{-1} (1 kick by each of 12 locusts) in the control group (P=0.0004, t=3.46, t-test) (Fig. 3B). From these velocities, the energy absorption in this rebound movement can be calculated: 78% in locusts treated with nail varnish compared with 88% in control locusts. In addition, the number of flexion and extension oscillations increased to an average of 5 after treatment from an average of 4 in control locusts.

Energy absorption by the buckling region

The forces required to induce 40 deg bends in the buckling region of the tibia were monitored experimentally using a servo-motor driven at velocities from 0.001 to 0.65 deg ms^{-1} (Fig. 4). Work loops derived from these movements allowed energy absorption by the buckling region to be monitored (Fig. 4B, see Materials and methods). At 0.001 deg ms^{-1} buckling, 871±253 μJ (10 locusts, 1 bend from each) of energy was stored, of which 212±33 μJ or 24% was returned when the tibia was restored to its natural shape.

A second bend applied 10 s after the first absorbed significantly less energy; 579±85 μJ (10 locusts, 1 bend from each), or around a 50% reduction (P=0.0036, w=144, U-test) (Fig. 5A). The energy released at stimulus offset on a second bend, 192±25 μJ, was not significantly less than the first (P=0.08, w=129, U-test). Additional repetitions of the buckling did not lead to further declines in the energy that could be stored. The original energy storage capacity returned gradually and was restored fully in 24 h, with no difference observed between the energy absorbed at the first bend and at 24 h (P=0.62, t=0.5, t-test). This indicates no permanent change to the structure of the buckling region (Fig. 5B) and is thus indicative of thixotropy (Barnes, 1997; Silver et al., 2002). To test for velocity-

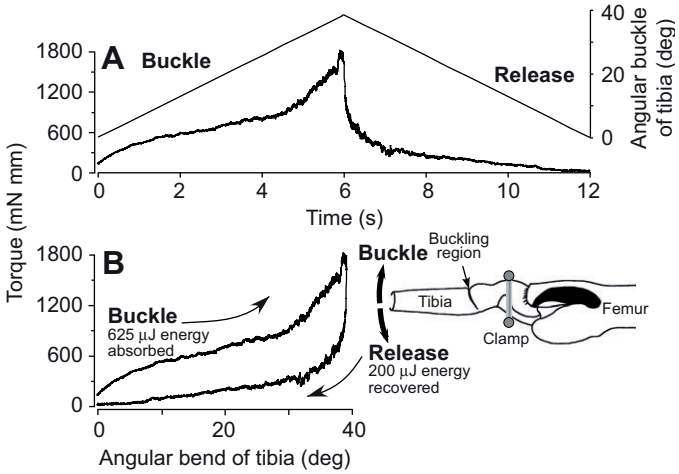

Fig. 4. Experimentally imposed movements of the tibia (see inset diagram) result in buckling. (A) Example plot from one locust of the torque resulting from an imposed bend and release of the tibia in a triangular waveform through 40 deg at a velocity of 0.0066 deg ms^{-1}. (B) The polynomial fit of the torques experienced during a bend and the subsequent release are plotted to provide a work loop relating torque to the bend at the buckling region. In this example, 625 µJ of energy was stored by the bend and 200 µJ was recovered on release.

dependent properties, we subjected the tibia to bends of several velocities. The first bend was discarded from our analysis to ensure that each tibia tested was in the same state, regardless of previous history of bending. Energy absorption was independent of the velocity of bending over the range tested (Fig. 5C).

Structure of the proximal tibia

Under incident white light, there was little to distinguish the buckling region from the surrounding tibia, unless it was bent. The buckling region occurs where the tibia is straight, just distal to a constriction on the dorsal surface (Figs 1, 2 and 6). Proximally, where the extensor and flexor tibiae muscles insert, the cuticle is sclerotised and black, but this gradually fades to a much lighter colouration at the buckling region and distal tibia, indicating that the cuticle is less stiff, with a lower Young's modulus (Vincent and Wegst, 2004). When the proximal tibia was illuminated with UV light of a specific and narrow band of wavelengths (see Materials and methods), the buckling region was clearly demarcated as a band of blue fluorescence (Fig. 6). At its widest point toward the dorsal and medial surface, the band was about 280 µm wide, tapering at its narrowest point to 120 µm (Fig. 6A,C,E). The band did not completely encircle the tibia and fluorescence was absent from the ventral surface (Fig. 6A,B). Sections made along the longitudinal axis of the tibia showed that fluorescence occurred on the dorsal (Fig. 6G), lateral and medial faces (Fig. 6H) of the tibia only at the buckling region, and again showed no fluorescence on the ventral surface (Fig. 6G). The fluorescence was sandwiched between thin layers of chitinous cuticle on all three faces of the tibia at the buckling region. In all preparations, fluorescence was dependent on pH, a second characteristic signature of resilin (Andersen, 1963; Neff et al., 2001). Resilin is likely to be cross-linked with other proteins in the cuticle (Qin et al., 2009).

When a force was applied to the tibia in the same direction experienced during natural jumping and kicking, buckling occurred precisely at the blue fluorescent band of the buckling region (Fig. 6B,D,F). When viewed from the lateral surface in the buckled

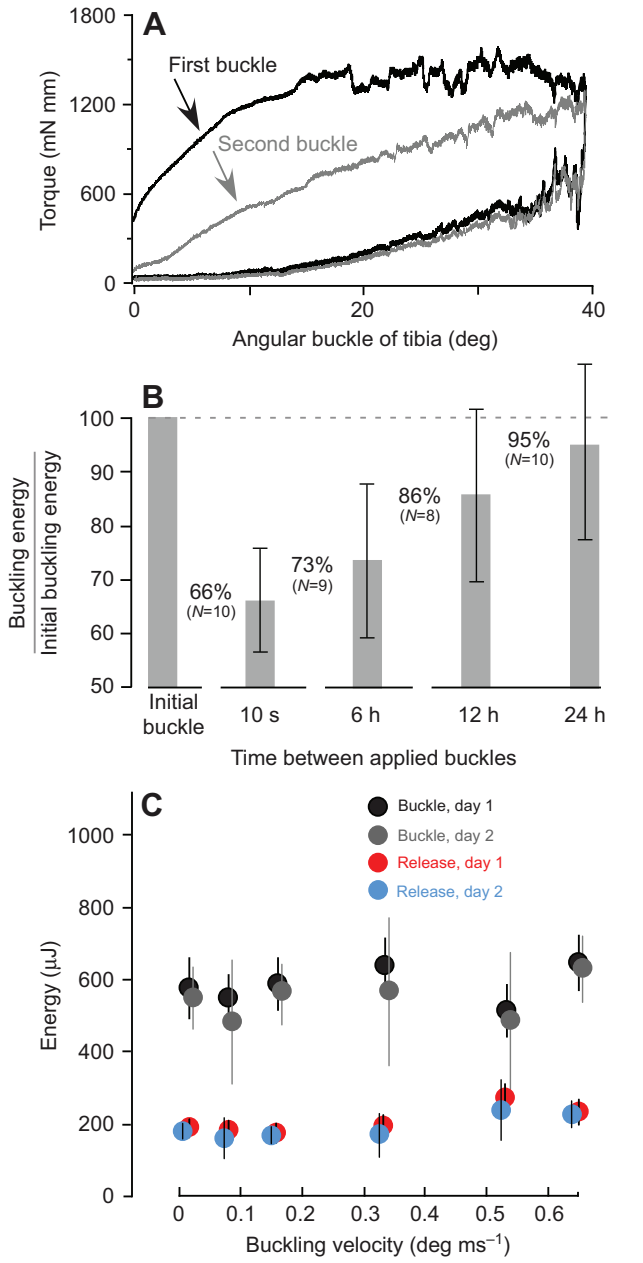

Fig. 5. Changes in energy storage by repeated bending of the buckling region. (A) Two example work loops for the first and second bends. The energy stored was lower on the second bend, but the energy recovered upon release remained the same. (B) Histograms to show the initial decline and subsequent recovery of the energy storage capacity when a second buckle was applied at 10 s, 6 h, 12 h and 24 h after the first. There was no difference between the energy absorbed on an initial bend and that absorbed on one presented after 24 h (P=0.62, t=0.5, t-test). (C) Repetitive buckling at different velocities. The energy stored and recovered was independent of velocity. The same sequence of bends, repeated 24 h later, gave the same energy on both bend and release.

position, the fluorescence separated into distal and proximal parts with a prominent V-shaped gap in the dorsal cuticle in between (Fig. 6B). When viewed dorsally, a proximal and lateral band of fluorescence overlapped with a distal and medial band (Fig. 6D). When viewed medially, the distal band of fluorescence had folded into the proximal band (Fig. 6F). Buckling thus involved a folding

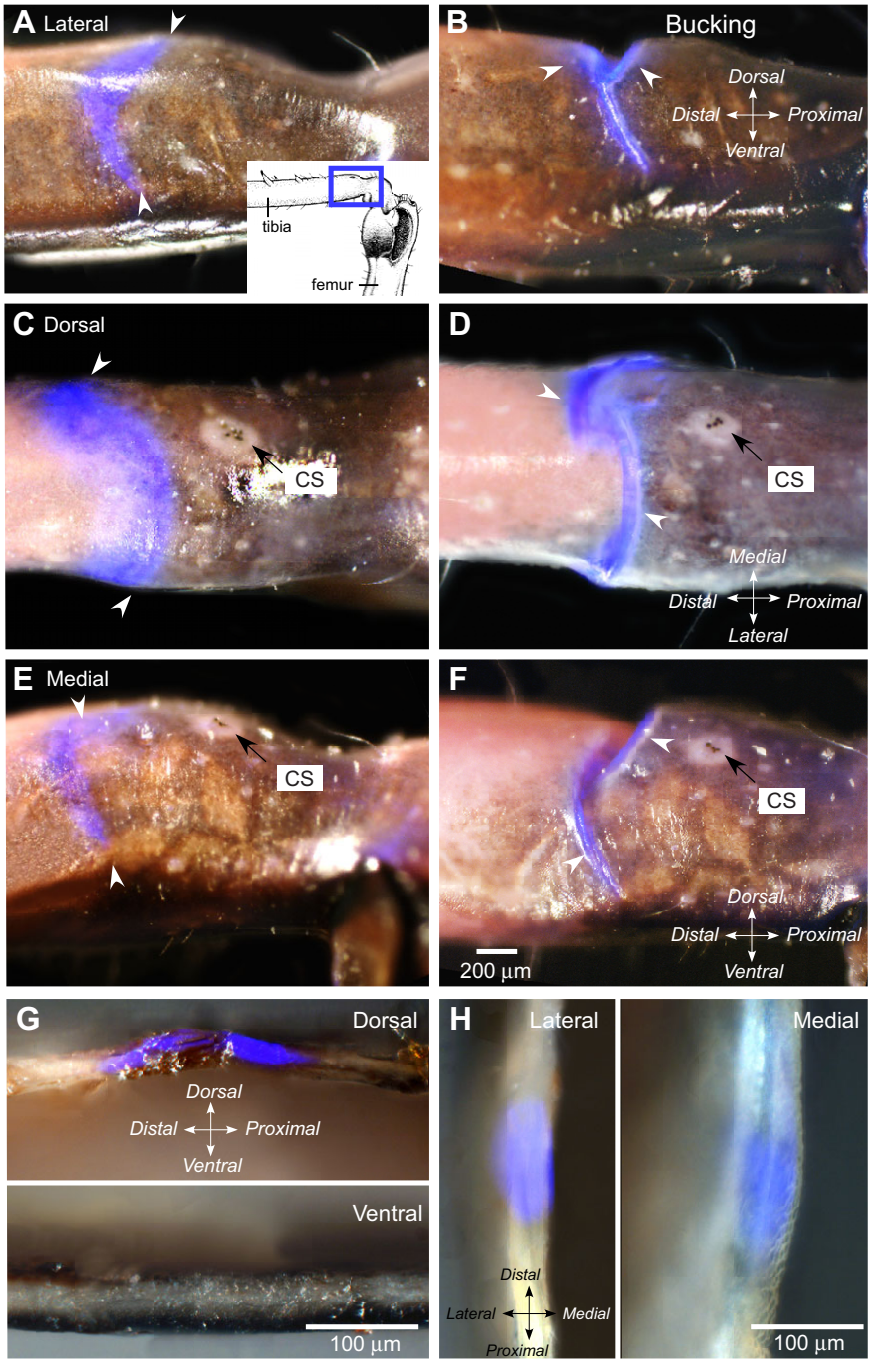

Fig. 6. The buckling region of the right hind-tibia viewed under white and UV illumination. The proximal tibia is shown extended (A,C,E) and buckled (B,D,F). The right tibia is viewed laterally (A,B), dorsally (C,D) and medially (E,F). Blue fluorescence indicating the presence of resilin at the buckling region is marked by white arrowheads. A group of campaniform sensilla (CS) proximal to the buckling region is indicated by black arrows in both dorsal and medial views. The inset to A shows a drawing of a medial view of the hind-FT joint with the area shown in the photographs outlined by the box. (G) A section cut from dorsal to ventral along the longitudinal axis of the tibia shows fluorescence between an outer and inner layer of chitinous cuticle at the dorsal surface of the buckling region. No fluorescence is present at the ventral surface of the buckling region. (H) A section along the same axis but cut from lateral to medial shows resilin on both the lateral and medial faces of the tibia only at the buckling region.

of the dorsal tibial cuticle at the region showing blue fluorescence, as also seen in scanning electron micrographs (Fig. 7A).

Campaniform sensilla at the buckling region

Around 300 µm proximal to the buckling region and on the dorso-medial surface is a prominent group of campaniform sensilla (Burrows and Pflüger, 1988) (Fig. 6C–F, Fig. 7A). There were 4–6 sensilla in the group (mean 5.2±0.7, 12 locusts, of which 8 had 5 sensilla). The longitudinal axis of the cap of a sensillum (Fig. 7B,C) had a mean length of 10.6±0.5 µm (7 locusts, 2 or 3 sensilla measured for each because several became blocked during fixation and their dimensions could not be measured). In the same group, the mean length of the transverse axis was 5.0±0.5 µm. The ratio of longitudinal/transverse axes did not vary between individuals (P=0.19, H=8.77, K–W), with the longitudinal axis being 2.2±0.6 times longer. This indicates a consistently ovoid shape of the caps of the sensilla. The longitudinal axes of the sensilla were aligned 11.7±1.5 deg clockwise from the long axis of the tibia and the range within each locust was 10.2±5.1 deg (7 locusts, 3–5 sensilla per locust). Thus, the sensilla appear to be approximately aligned parallel to the longitudinal axis of the tibia and perpendicular to the buckling region. No function for these sensilla has been established (Heitler and Burrows, 1977b) although it has been suggested that they may respond to buckling of the tibia at the buckling region (Heitler, 1977).

To test whether these campaniform sensilla do respond to buckling, the tibia was bent at velocities and amplitudes of buckling similar to those observed in preparation for kicks when full flexion of the tibia about the femur was impeded. A typical response is

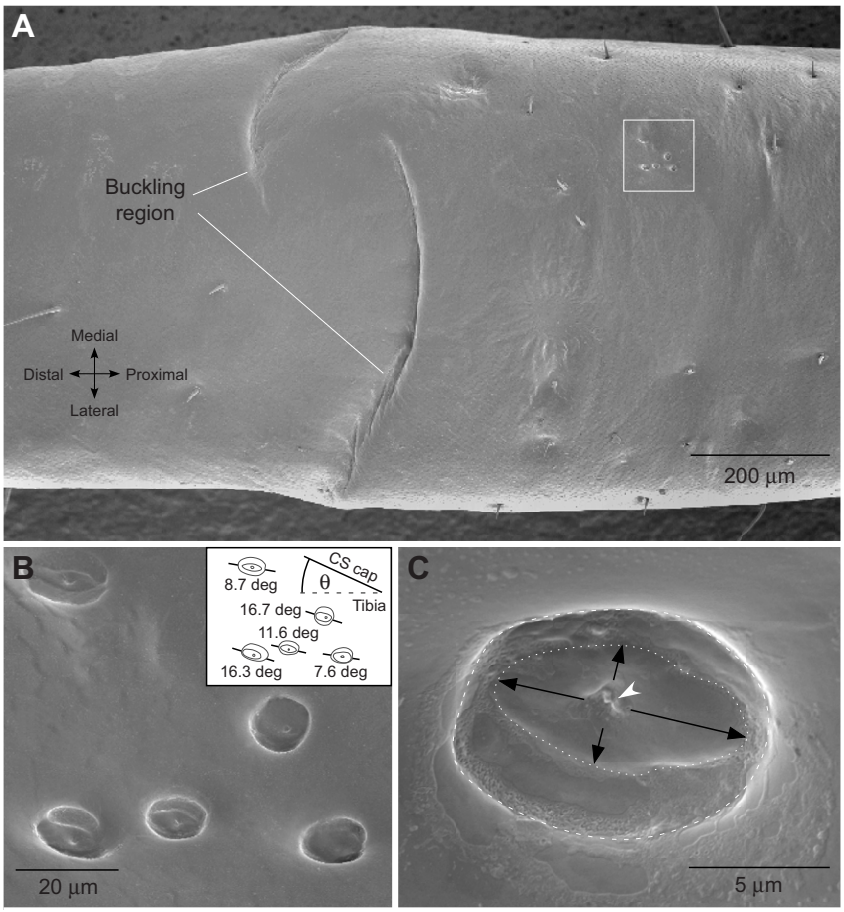

Fig. 7. Scanning electron micrographs of the buckling region and adjacent sensory structures. (A) Dorsal view of a right hind-tibia. Two cuticular folds are visible at the buckling region and toward the medial side is a group of campaniform sensilla (box). Although the tibia is not bent, and so the buckling region would normally not be visible, the soft cuticle is likely to have deformed during fixation. (B) Higher power image of the group of sensilla. The angle (θ) of the long axes of the campaniform sensilla to the long axis of the tibia is indicated in the inset. (C) An individual sensillum at higher magnification. The cap (dotted white line) and pit (dashed white line) of the sensillum are outlined. Black arrows indicate the longitudinal and transverse axes of the cap, and the white arrowhead shows the point through which the nerve innervating the sensillum has migrated during a moult (Moran et al., 1971).

shown to one bend (Fig. 8A). The higher velocities that occur at the end of a kick were beyond the limit of our servo-motor, but velocities up to 0.3 deg ms^{-1} all elicited spikes. Spikes of three distinct amplitudes were reliably elicited (denoted units 1, 2 and 3 in order of decreasing amplitude). The reason we could reliably recognise only 3 spike shapes but an average of 5 sensilla was unclear. The spiking was in clear contrast to the lack of response to tibial movements in which buckling did not occur. For all statistics given below, significance was adjusted by the Bonferroni–Dunn procedure to control for multiple comparisons, giving values equivalent to $P<0.05$ at $P<0.0025$; $P<0.01$ at $P<0.0005$; and $P<0.001$ at $P<0.00005$.

Unit 1 (the largest spike amplitude) (Fig. 8B) was silent at rest, most active when the tibia was being bent, and spiked only sporadically on sustained tibial bending or release. The response to the ramp was significantly different from lead-in ($P<0.00005$, $Z=5.44$, K–W), hold ($P=0.0013$, $Z=3.22$, K–W), release ($P=0.0003$, $Z=3.22$, K–W) and lead-out ($P=0.0002$, $Z=3.72$, K–W). Of the 5 locusts tested, three showed an increase in spike rate at stimulus onset as the amplitude of buckling increased from 2 to 4 deg ($P=0.02$, $t=4.3$, t-test), but then reached saturation (Fig. 9C). Two individuals showed no change in spike rate with amplitude. The spike rate of unit 1 was similar over the range of velocities tested (not shown). This unit thus can signal the onset of tibial buckling.

Unit 2 (the intermediate spike amplitude) again showed its strongest response to stimulus onset (Fig. 8C), which differed from the lead-in ($P<0.00005$, $Z=4.95$, K–W) and lead-out sections ($P=0.0001$, $Z=4.03$, K–W). The response to sustained bending ($P=0.00051$, $Z=2.80$, K–W) and release ($P=0.00085$, $Z=2.63$, K–W) differed from rest (lead-in). Unit 2 showed a rise in spike rate with velocity on stimulus onset, reaching a peak at around 0.01 deg ms^{-1} (Fig. 9D). Its response on the release stimulus was independent of velocity. It showed no sensitivity to changes in amplitude. This neuron can therefore signal that the tibia is buckling.

Unit 3 (the smallest spike amplitude) spiked tonically when the leg was clamped and when it was returned to its straight position and adapted after 30 s. It showed a clearly modulated response when the tibia buckled (Fig. 8A), but the response was not reliable and no significant trends arose on averaging between individuals (Fig. 8D). It did, however, show a significant increase in spike rate at stimulus onset with increasing amplitude of bending, reaching a peak at around 16 deg (Fig. 9E). It showed no change in spike rate with increasing velocity. This neuron can therefore signal the amplitude of buckling.

DISCUSSION

We have provided evidence for the proposals of Heitler (Heitler, 1977) for the following functions of the buckling region. First, the inertial shock of a kick that misses its target is reduced by the absorption of kinetic energy at the buckling region as it bends through 32 deg at a rate of 33 deg ms^{-1} (Fig. 3B). Second, if flexion is impeded in preparation for a jump or a kick, the buckling region allows the tibia to flex fully about the femur, by bending through 9 deg at 0.063 deg ms^{-1}. Third, a nearby group of campaniform sensilla respond to bending of the buckling region (Figs 8, 9). In addition, we have shown that the buckling region bends by 23 deg at 13 deg ms^{-1} when a hindleg of a locust slips during jumping (Fig. 1). We found a band of the rubber-like protein resilin, as

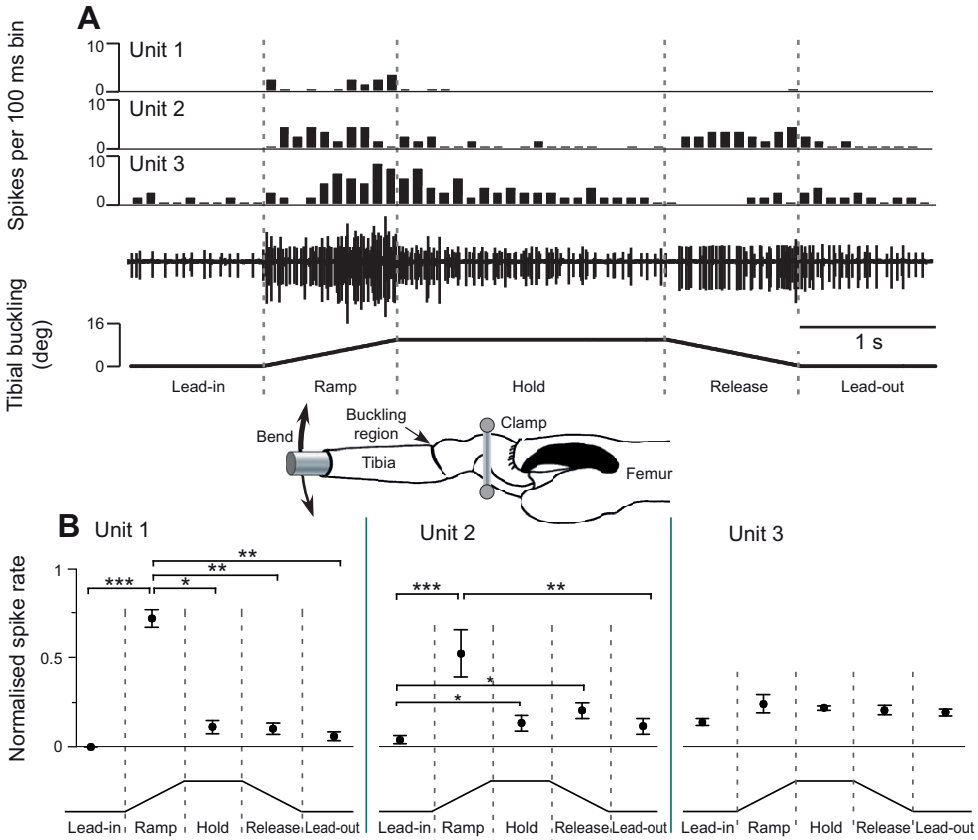

Fig. 8. Responses of campaniform sensilla to tibial buckling. (A) Example trace from one locust of a ramp-and-hold extension of the tibia by 10 deg at 0.01 deg ms^{-1}. The bars represent the mean spike rate per 100 ms bin on three bends of the tibia (separated by 5 min) for one of the 5 locusts analysed. (B,C,D) Normalised spike rates of the three units identified by their spike amplitude, to a ramp-and-hold stimulus (5 locusts, 3 bends per locust). The inset diagram shows how the tibia was clamped proximal to the group of campaniform sensilla and attached distally to the moving device that caused buckling. Significance was adjusted by the Bonferroni–Dunn procedure to $*P<0.0025$, $**P<0.0005$ and $***P<0.00005$ (Kruskal–Wallis).

indicated by blue fluorescence under UV illumination, on the dorsal, lateral and medial surfaces of the buckling region, which had not been reported previously (Heitler, 1977) (Fig. 6). Calculations from buckling imposed on the tibia, at velocities similar to those recorded during the preparatory phase of a kick, show that the buckling region can absorb energy equivalent to half that expended in a kick (Fig. 5).

What role does tibial buckling play?

All animals must respond to unexpected perturbations of natural movements. In cats, neural mechanisms in the brain (Gorassini et al., 1994) and spinal cord (Hiebert et al., 1994) play a key role in adjusting perturbed locomotion. In guinea fowl, neural compensation is aided by specialisations in the musculature during running (Biewener and Daley, 2007; Daley et al., 2009). In cockroaches, a combination of neural and passive musculo-skeletal compensatory mechanisms has been suggested to be used (Jindrich and Full, 2002; Dudek and Full, 2006). As first suggested by Heitler (Heitler, 1977), and supported by evidence in this paper, locusts use their tibial buckling region to absorb excess kinetic energy during a range of movements, and this further underlines the importance of skeletal mechanisms in the control of movement.

A kick by a single hindleg produces about 1700 μJ of energy, whereas a jump powered by both legs produces 4100–4800 μJ. As the tibia reaches full extension during a jump or a kick, the maximum bending moment will be at its articulation with the femur. The buckling region is located just distal to this joint where it can dissipate 88% of the kinetic energy of a kick. When buckling was prevented experimentally, about 78% of the kinetic energy was still absorbed. We were unable to detect differences in kick velocity over a sequence of 5 kicks, indicating no damage to the machinery occurred. This suggests either that the varnish absorbed energy, or that other structures, such as the more proximal joints of the leg, are involved.

The amount of energy absorbed by the buckling region was tested directly by imposing movements at velocities recorded during the preparatory phase of some jumps. The very high velocities during the extension phase of a jump or a kick could not be replicated because of the mechanical limitations of our servo-motors. Around 850 μJ of energy was absorbed on the first applied buckle and 600 μJ on subsequent repeated buckles. The initial energy-absorbing properties returned within 24 h (Fig. 5B), a time scale that is shorter than that of the healing process in arthropods, which can take days to weeks (Galko and Krasnow, 2004; Jeong and Moon, 1997). This implies thixotropic mechanical properties (Barnes, 1997; Fung, 1993), which are common in biological structures (e.g. Silver et al., 2002). Within the range of velocities measured we detected no change in energy absorption by the buckling region, and so our slower bends are likely only to measure its elastic properties (Fig. 5C). As such, these movements may not have been sufficiently fast to measure its frictional viscous or visco-elastic properties (Fung, 1993). The values of these properties can only increase with increasing velocity, implying that the buckling region can absorb more energy during natural jumping and kicking than we have calculated from our slower imposed buckling. Similarly, in other arthropods where movements occur this quickly, slow bends of the structures have been used as proxies for the energy storage capabilities of cuticle during faster natural movements (Zack et al., 2009).

Is the blue fluorescence from resilin?

The only tests to identify resilin currently available are of the properties of its fluorescence (Andersen and Weis-Fogh, 1964; Burrows et al., 2008; Neff et al., 2001). First, the intense blue fluorescence was only visible when viewed with emission filters that transmitted wavelengths from 413 to 483 nm. With other

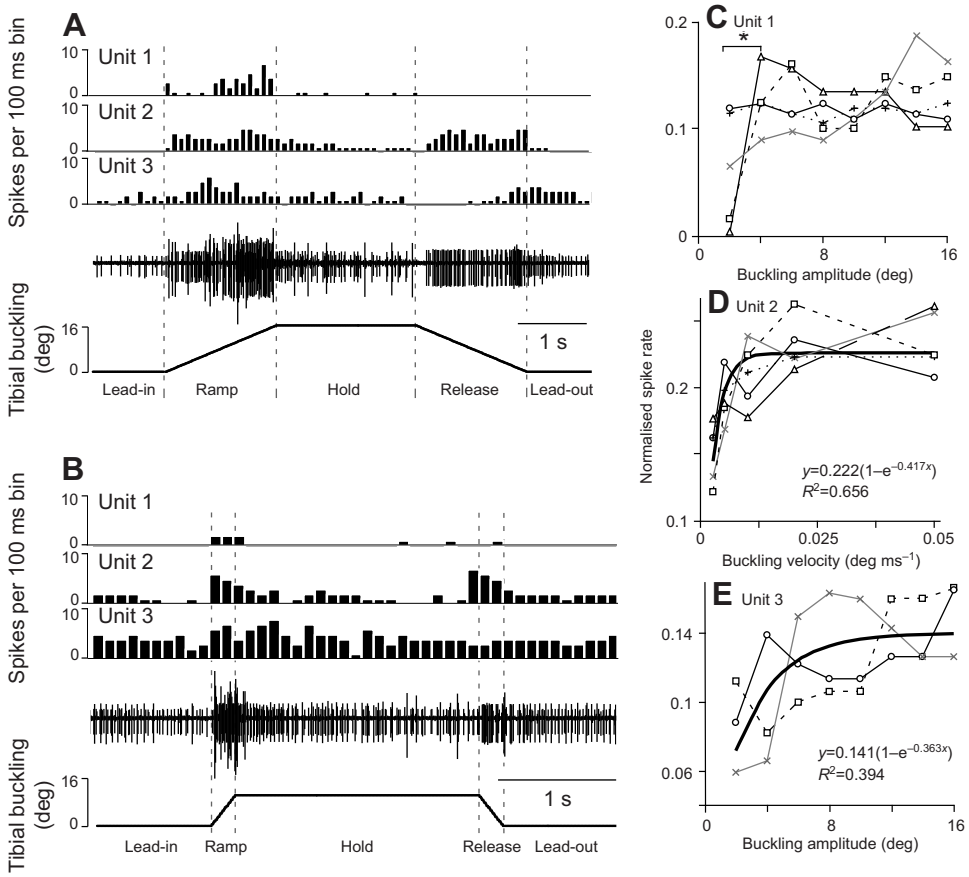

Fig. 9. Responses of campaniform sensilla to different velocities and amplitudes of tibial buckling. (A) 16 deg extension at a rate of 0.01 deg ms^{-1}. (B) 10 deg extension at a rate of 0.05 deg ms^{-1}.The spike rates of the three units identified by their amplitudes during the different phases of the stimulus are displayed in 100 ms bins. (C,D,E) Spike responses of the three units that changed significantly with either velocity or amplitude. The responses of individual locusts are represented by different symbols. (C) Three locusts show an increase in the spike rate of unit 1 with an amplitude between 2 and 4 deg (P=0.02, t=4.3, t-test, 3 bends per locust), but did not show any further increase with amplitude. Two had a similar range of spike rates across all amplitudes tested. (D) In all 5 locusts tested, the spike rate of unit 2 increased exponentially with velocity (3 bends per locust). (E) In the three locusts tested, the spike rate of unit 3 increased exponentially with amplitude (3 bends per locust). Exponential fits are shown as thick black lines for D and E; significance was tested by an ANOVA of residuals, P<0.05.

emission filters (for example, CY3 and GFP), no fluorescence was detected. Second, resilin fluorescence has reversible sensitivity to pH, which was observed here. A recently introduced resilin antibody should add a further means of identification in future studies (Burrows et al., 2011; Lyons et al., 2011).

What could be the role of resilin at the buckling region? Its elastic properties could be involved in the storage of energy as the tibia is buckled. Resilin in froghoppers stores only 1–2% of the energy required for a jump, while the rest is stored in the stiffer chitinous cuticle with which it forms a composite structure (Burrows et al., 2008). Resilin may prevent the harder cuticle from fracturing and allow the distorted structure to return quickly to its original shape (Burrows et al., 2008). At the buckling region, the restoration of the shape of the tibia is likely to be important, as it could allow a locust to kick a target after missing on an initial attempt, or to jump again after one jump has failed.

Campaniform sensilla monitor tibial buckling

In termites, a tibial plane of weakness is suggested to focus forces generated by leg movements on a group of campaniform sensilla (Howse, 1965). In the locust tibia analysed here, the sensory neurons of the group of campaniform sensilla close to the buckling region responded to imposed buckling and collectively coded the onset and maintenance of its deformation. No response was recorded in these experiments unless buckling was induced. What effects on the motor circuitry might be expected from these sensilla?

Individual campaniform sensilla separate from, but close to, the group analysed here respond to strain in the proximal tibia, and make direct excitatory connections with the fast extensor and some fast flexor motor neurons (Burrows and Pflüger, 1988). These connections create a positive feedback loop that increases the force generated by the extensor tibiae muscle during co-contraction with the flexor tibiae muscle in preparation for a jump or kick. A previous survey of sensory neurons on the hindleg of a locust could not identify an effect of the group of sensilla analysed here on hindleg motor neurons (Heitler and Burrows, 1977b).

The time from the initiation of sensory signals in the group of campaniform sensilla to the start of a muscle contraction would be 30–40 ms. These figures are calculated from the known spike conduction times of 15–30 ms of neighbouring individual campaniform sensilla to the metathoracic ganglion (Burrows and Pflüger, 1988), the likely processing time in the metathoracic ganglion (2–4 ms depending on the number of synapses involved), and the conduction times of motor spikes to the femoral muscles (5–10 ms depending on axon diameter) (Gwilliam and Burrows, 1980; Pearson et al., 1970). To effect a change in muscle tension would considerably increase this period. This means that the sensory signals could affect muscular forces and hence buckling that occurs if the preparatory phase of a jump or kick is impeded. There is, however, insufficient time for these sensory signals to produce an effect either on the buckling that occurs during extension of the tibia in a kick (all over in 5 ms) or in a jump (all over in 20–30 ms). Perhaps the sensory signals influence subsequent movements by reducing the force generated in the next jump or kick to allow for recovery from the first tibial buckle. Although these sensilla clearly do respond to buckling, this does not exclude the possibility that they also act during other movements that have not been studied here.

ACKNOWLEDGEMENTS

The main body of this work was carried out by T.G.B. as part of an undergraduate project. We thank Jo Riley for her invaluable help and Steve Shaw at Dalhousie

University, Halifax, NS, Canada, Hillel Chiel at Case Western Reserve University, Cleveland, OH, USA, and Cambridge colleagues for their many constructive suggestions on the manuscript.

FUNDING

G.P.S. was funded by the Marshall Sherfield Commission and the Human Frontiers Research Program.

REFERENCES

Andersen, S. O. (1963). Characterization of a new type of cross-linkage in resilin, a rubber-like protein. *Biochim. Biophys. Acta* **69**, 249-262.
Andersen, S. O. and Weis-Fogh, T. (1964). Resilin. A rubberlike protein in arthropod cuticle. *Adv. Insect Physiol.* **2**, 1-65.
Barnes, H. A. (1997). Thixotropy – a review. *J. Non-Newtonian Fluid Mech.* **70**, 1-33.
Bennell, K. L. and Brukner, P. D. (1997). Epidemiology and site specificity of stress fractures. *Clin. Sports Med.* **16**, 179-192.
Bennell, K. L. and Brukner, P. (2005). Preventing and managing stress fractures in athletes. *Phys. Ther. Sport* **6**, 171-180.
Bennet-Clark, H. C. (1975). The energetics of the jump of the locust *Schistocerca gregaria*. *J. Exp. Biol.* **63**, 53-83.
Biewener, A. A. and Daley, M. A. (2007). Unsteady locomotion: integrating muscle function with whole body dynamics and neuromuscular control. *J. Exp. Biol.* **210**, 2949-2960.
Branch, T., Clyde, P., Chamberland, P., Emeterio, E. and Sabetelle, M. (1991). Spontaneous fractures of the humerus during pitching: a series of 12 cases. *Am. J. Sports Med.* **20**, 468-470.
Brown, R. H. J. (1967). The mechanism of locust jumping. *Nature* **214**, 939.
Burrows, M. (2003). Froghopper insects leap to new heights. *Nature* **424**, 509.
Burrows, M. (2006). Jumping performance of froghopper insects. *J. Exp. Biol.* **209**, 4607-4621.
Burrows, M. (2009). Jumping performance of planthoppers (Hemiptera, Issidae). *J. Exp. Biol.* **212**, 2844-2855.
Burrows, M. and Morris, G. (2001). The kinematics and neural control of high speed kicking movements in the locust. *J. Exp. Biol.* **204**, 3471-3481.
Burrows, M. and Pflüger, H. J. (1988). Positive feedback loops from proprioceptors involved in leg movements of the locust. *J. Comp. Physiol. A* **163**, 425-440.
Burrows, M., Shaw, S. R. and Sutton, G. P. (2008). Resilin and cuticle form a composite structure for energy storage in jumping by froghopper insects. *BMC Biol.* **6**, 41.
Burrows, M., Borycz, J. A., Shaw, S. R., Elvin, C. M. and Meinertzhagen, I. A. (2011). Antibody labelling of resilin in energy stores for jumping in plant sucking insects. *PLoS ONE* **6**, e28456.
Daley, M. A., Voloshina, A. and Biewener, A. A. (2009). The role of intrinsic muscle mechanics in the neuromuscular control of stable running in the guinea fowl. *J. Physiol.* **587 11**, 2693-2707.
Dudek, D. M. and Full, R. J. (2006). Passive mechanical properties of legs from running insects. *J. Exp. Biol.* **209**, 1502-1515.
Fung, Y. C. (1993). *Biomechanics: Mechanical Properties of Living Tissue*, 568pp. New York: Springer.
Galko, M. J. and Krasnow, M. A. (2004). Cellular and genetic analysis of wound healing in *Drosophila* larvae. *PLoS Biol.* **2**, e239.
Gorassini, M. A., Prochazka, A., Herbert, G. W. and Gauthier, J. A. (1994). Corrective responses to loss of ground support during walking. I. Intact cats. *J. Neurophysiol.* **71**, 603-610.
Gwilliam, G. F. and Burrows, M. (1980). Electrical characteristics of the membrane of an identified insect motor neurone. *J. Exp. Biol.* **86**, 49-61.
Heitler, W. J. (1977). The locust jump. III. Structural specializations of the metathoracic tibiae. *J. Exp. Biol.* **67**, 29-36.
Heitler, W. J. and Burrows, M. (1977a). The locust jump. I. The motor programme. *J. Exp. Biol.* **66**, 203-219.
Heitler, W. J. and Burrows, M. (1977b). The locust jump. II. Neural circuits of the motor programme. *J. Exp. Biol.* **66**, 221-241.
Hiebert, G. W., Gorassini, M. A., Jiang, W. and Prochazka, A. (1994). Corrective responses to loss of ground support during walking. II. Comparison of intact and chronic spinal cats. *J. Neurophysiol.* **71**, 611-622.
Hillerton, J. E., Reynolds, S. E. and Vincent, J. F. V. (1982). On the indentation hardness of insect cuticle. *J. Exp. Biol.* **96**, 45-52.
Howse, P. E. (1965). The structure of the subgenual organ and certain other mechanoreceptors of the termite *Zootermpsis angusticollis* (Hagen). *Proc. R. Ent. Soc. Lond.* **40**, 137-146.
Jeong, M.-J. and Moon, M.-J. (1997). Fine structure of the integumentary wound healing process in the spider *Pardosa astrigera*. *Korean J. Entomol.* **27**, 29-41.
Jindrich, D. L. and Full, R. J. (2002). Dynamic stabilization of rapid hexapedal locomotion. *J. Exp. Biol.* **205**, 2803-2823.
Jones, G. L. (2006). Upper extremity stress fractures. *Clin. Sports Med.* **25**, 159-174.
Lyons, R. E., Wong, D. C. C., Kim, M., Lekieffre, N., Huson, M. G., Vuocolo, T., Merritt, D. J., Nairn, K. M., Dudek, D. M., Colgrave, M. L. et al. (2011). Molecular and functional characterisation of resilin across three insect orders. *Insect Biochem. Mol. Biol.* **41**, 881-890.
Moran, D. T., Chapman, K. M. and Ellis, R. A. (1971). The fine structure of cockroach campaniform sensilla. *J. Cell Biol.* **48**, 155-173.
Neff, D., Frazier, S. F., Quimby, L., Wang, R.-T. and Zill, S. (2001). Identification of resilin in the leg of cockroach, *Periplaneta americana:* confirmation by a simple method using pH dependence of UV fluorescence. *Arthropod Struct. Dev.* **29**, 75-83.
Pearson, K. G., Stein, R. B. and Malhotra, S. K. (1970). Properties of action potentials from insect motor nerve fibres. *J. Exp. Biol.* **53**, 299-316.
Pohl, M. B., Mullineaux, D. R., Milner, C. E., Hamill, J. and Davis, I. S. (2008). Biomechanical predictors of retrospective tibial stress fractures in runners. *J. Biomech.* **41**, 1160-1165.
Polu, K. R., Schenck, R. C. J., Wirth, M. A., Greeson, J., Cone, R. O. I. and Rockwood, C. A. J. (1999). Stress fracture of the humerus in a collegiate baseball pitcher: a case report. *Am. J. Sports Med.* **27**, 813-816.
Qin, G., Lapidot, S., Numata, K., Hu, X., Meirovitch, S., Deke, M., Podoler, I., Shoseyov, O. and Kaplan, D. L. (2009). Expression, cross-linking, and characterization of recombinant chitin binding resilin. *Biomacromolecules* **14**, 3227-3234.
Sabick, M. B., Torry, M. R., Kim, Y.-K. and Hawkins, R. J. (2004). Humeral torque in professional baseball pitchers. *Am. J. Sports Med.* **32**, 892-898.
Silver, F. H., Ebrahimi, A. and Snowhill, P. B. (2002). Viscoelastic properties of self-assembled type 1 collagen fibers: molecular basis of elastic and viscous behaviors. *Connect. Tissue Res.* **43**, 569-580.
Spinola, S. M. and Chapman, K. M. (1975). Proprioceptive indentation of the campaniform sensilla of cockroach legs. *J. Comp. Physiol.* **96**, 257-272.
Usherwood, P. N. R. and Grundfest, H. (1965). Peripheral inhibition in skeletal muscle of insects. *J. Neurophysiol.* **28**, 497-518.
Vincent, J. F. V. and Wegst, U. G. K. (2004). Design and mechanical properties of insect cuticle. *Arthropod Struct. Dev.* **33**, 187-199.
Zack, T. I., Claverie, T. and Patek, S. N. (2009). Elastic energy storage in the mantis shrimp's fast predatory strike. *J. Exp. Biol.* **212**, 4002-4009.